

Charge state of metal atoms on oxide supports: a systematic study based on simulated infrared spectroscopy and density functional theory

Antonio M. Márquez · Jesús Graciani ·
Javier Fdez Sanz

Received: 27 July 2009 / Accepted: 18 November 2009 / Published online: 11 December 2009
© Springer-Verlag 2009

Abstract A long standing question in the study of supported clusters of metal atoms in the properties of metal–oxide interfaces is the extent of metal–oxide charge transfer. However, the determination of this charge transfer is far from straight forward and a combination of different methods (both experimental and theoretical) is required. In this paper, we systematically study the charging of some adsorbed transition metal atoms on two widely used metal oxides surfaces [α -Al₂O₃ (0001) and rutile TiO₂ (110)]. Two procedures are combined to this end: the computed vibrational shift of the CO molecule, that is used as a probe, and the calculation of the atoms charges from a Bader analysis of the electron density of the systems under study. At difference from previous studies that directly compared the vibrational wavenumber of adsorbed CO with that of the gas phase molecule, we have validated the procedure by comparison of the computed CO stretching wavenumbers in isolated monocarbonyls (MCO) and their singly charged ions with experimental data for these species in rare gas matrices. It is found that the computational results correctly reproduce the experimental trend for the observed shift on the CO stretching mode but that care must be taken for negatively charged complexes as in this case there is a significative difference between the total charge of the MCO complex and the charge of the M atom.

For the supported adatoms, our results show that while Cu and Ag atoms show a partial charge transfer to the Al₂O₃ surface, this is not the case for Au adatoms, that are basically neutral on the most stable adsorption site. Pd and Pt adatoms also show a significative amount of charge transfer to this surface. On the TiO₂ surface our results allow an interpretation of previous contradictory data by showing that the adsorption of the probe molecule may repolarize the Au adatoms, that are basically neutral when isolated, and show the presence of highly charged Au ^{$\delta+$} –CO complexes. The other two coinage metal atoms are found to significantly reduce the TiO₂ surface. The combined use of the shift on the vibrational frequency of the CO molecule and the computation of the Bader charges shows to be an useful tool for the study the charge state of adsorbed transition metal atoms and allow to rationalize the information coming from complementary tools.

Keywords Copper · Silver · Gold · Palladium · Platinum · Aluminum oxide · Titanium oxide · Adsorption · Density functional calculations · Charge state

1 Introduction

Deposition of metal atoms and clusters on the surface of oxide materials is a topic that has been extensively studied for a long time. The several technological applications of metal–oxide interfaces, ranging from microelectronics to catalysis, make the field one of the most active in surface science and technology research [1–16]. In recent years, very accurate ultrahigh vacuum (UHV) experimental techniques have been developed to gain insight into the properties and structure of small metal aggregates on oxide surfaces. Samples may be characterized by, e.g. scanning

Dedicated to the memory of Professor Jean-Pierre Daudey and published as part of the Daudey Memorial Issue.

A. M. Márquez (✉) · J. Graciani · J. F. Sanz
Departamento de Química Física, Facultad de Química,
Universidad de Sevilla, CL/Prof. García González, 1,
41012 Sevilla, Spain
e-mail: marquez@us.es

tunneling microscopy (STM), atomic force microscopy (AFM), transmission electron microscopy (TEM), and infrared reflection absorption spectroscopy (IRAS), between other techniques [17]. However, while an atomic level understanding of the surface structure and electronic properties is desirable, it is far from straightforward. Analysis of experimental data alone is not, in general, sufficient to provide a well grounded hypothesis about the microscopic structure of the adsorption site. In this regard, the combination of experiment with well calibrated first principles theoretical calculations is proving to be a useful strategy to understand the chemistry and physics of these complex systems.

A long standing question in the study of supported clusters of metal atoms in the properties of metal–oxide interfaces is the extent of metal–oxide charge transfer. This question is of the maximum relevance as the amount of metal–support interaction and catalytic activity are highly related to the amount and direction of metal–support charge transfer (see, for example [2–11] and references in these papers). Adsorption of small molecules on deposited metal atoms, clusters, or nanoparticles, provides very useful, although indirect, information about the metal adsorption site, electronic structure, and modifications of the metal–oxide interface. IRAS of small probe molecules has shown to be a valuable means to identify particular binding sites on the surface of the supported metal particle. Although the data from these experiments may not directly define the properties of the surface, they can differentiate the behavior of different surface sites. The position and intensities of vibrational band of adsorbed CO can give useful information about the interaction energy of the CO molecule with the probed site [17, 18]. The magnitude of this shift can, in principle, be used to measure the electrostatic field strength surrounding the TM atom and, thus, as an indirect measure of the charge of the adsorbed TM atom. DFT calculations can provide the vibrational frequencies of CO adsorbed to metal atoms deposited on oxide surfaces but to be used as a quantitative tool to determine the metal charge the procedure must be validated against systems of known charge and/or other means of computation of the metal charge [6, 12–14]. In a recent paper, Frank et al. [6] using CO as a probe molecule, have shown that IR spectroscopy may provide valuable data both on structure and charge of small aggregates and single metal atoms supported on oxides surfaces. In particular, the relation between the charge state of Au particles and the shift on the CO stretching frequency has been the subject of different works with conflicting results. Initial studies on free and MgO supported AuCO complexes [15, 16] claimed, both from experimental and theoretical view points, that the probe molecule may

change the oxidation state reported for the adsorbed adatoms. However, more recent work by Bagus and Pacchioni [19], that have analyzed the different contributions to the bonding and vibrational frequency shifts for CO adsorbed on neutral, cationic, and anionic gold clusters, concluded that computational results correctly reproduce the trends observed experimentally.

Unsaturated transition metal (TM) carbonyls have been the subject of a large number of theoretical works, most of which are centered on monocarbonyls with a variety of methods being used. Generally, these calculations have focused on equilibrium geometries, harmonic frequencies, and binding energies (see [20] and references therein). While these studies have provided important insight into the bonding mechanism, only the more recent density functional (DFT) calculations have provided a consistent set of vibrational frequencies for these systems.

Aluminum oxide (Al_2O_3) is an important substrate for catalysis due to its thermal and mechanical resistance. Many experimental studies in the literature have been dedicated to study the growth and binding of metal particles on various alumina surfaces (see [2, 5] and references therein). In addition to these experimental efforts, many theoretical studies have examined metal adsorption on $\alpha\text{-Al}_2\text{O}_3$ surfaces [8–11, 21–27]. Analysis of the metal–surface bond shows different behavior depending on the electronic structure of the TM atom. For instance, periodic DFT calculations at low coverage ($\theta = 1/3$ ML, the smallest one can reach with a 1×1 cell) show that Pd atoms bind the surface on top of the oxygen atoms. Further analysis of the interaction, based on cluster models calculations and constrained space orbital variation (CSOV) analysis [28–30] of the interaction energy, indicate that the main contribution to the bonding comes from metal polarization and surface relaxation, with little charge transfer. [8] Similar results were obtained in a different study by Rivanenkov et al. [23] for the bonding mechanism of Pd and Pt atoms to the $\alpha\text{-Al}_2\text{O}_3$ (0001) surface. The authors found that a significant amount of the adsorption energy is due to substrate relaxation and no indication was found of the oxidation of Pd or Pt. A lot of research has been dedicated to the coinage metal atoms/TM oxide systems due to the high activity catalytic properties of dispersed gold nanoparticles. In the case of the $\alpha\text{-Al}_2\text{O}_3$ (0001) surface, DFT calculations, reveal that the interaction is relatively weak, with binding energies ranging between -0.6 and -1.1 eV, following the order $\text{Cu} > \text{Au} > \text{Ag}$. Analysis of density of states and of the different contributions to the bonding, based again in cluster models and CSOV decomposition of the interaction energy, indicates that there is a change in bonding mechanism going down the

group [10]. Cu atoms clearly reduce the surface, more specifically the outermost Al atoms, being this charge transfer to the surface the main contribution to the bonding, with some contribution from TM atom polarization. In the case of Ag, and Au atoms, while the charge transfer contribution is similar, but smaller than in the case of Cu, there is an increasing contribution from the TM atom polarization, being dominated the bonding energy by this mechanism in the case of Au. The TM/TiO₂ have received special attention as the activity of these catalysts is exceptionally high when the TM is supported on reducible oxides. DFT calculations have been extensively used to provide information on the adsorption site, geometric and electronic structure of small TM aggregates on the rutile TiO₂ (110) surface. Earliest DFT calculations concentrated on the adsorption of single coinage metal atoms trying to identify the nature of the bonding between these metal atoms and the rutile surface [31, 32]. It was found that Cu and Ag give rise to strong adsorption with nearly full electron transfer from the metal to the surface. However, the picture of the bonding is quite different for Au, with only minor charge transfer and a polarization of the metal to the surface O atoms. The number of theoretical studies devoted to the Pd/TiO₂ and Pt/TiO₂ systems is relatively scarce [33, 34]. For Pd/TiO₂ picture of the bonding in this system corresponds to the interaction of the Pd atom with two in-plane oxygens, a fivefold Ti atom and a protruding oxygen, with predominance of the TM polarization in the bonding mechanism [33]. Details of the bonding mechanism in the Pt/TiO₂ system have not been unveiled yet.

In this work, we present a systematic theoretical study by means of first principles density functional theory calculation of the shift in the vibrational frequency of one usual probe molecule (CO) when interacting with different transition metal atoms or their ions. First, we will validate the method by examining the existing correlation between the CO stretching frequency in mononuclear MCO complexes (M = Cu, Ag, Au, Pd, and Pt) and the charge of the complex. The results obtained show that there is a linear correlation between the computed shift in the vibrational frequency of the probe molecule and the charge of the probed metal atom. Later, we will compute the vibrational frequency of CO adsorbed to single TM atoms supported on two commonly used oxide materials: α -Al₂O₃, and rutile TiO₂. The computed CO stretching frequency will be used to determine, by using the above mentioned correlation with the charge in MCO complexes, the charge of the adsorbed TM atom. The results will be compared to atomic charges obtained from a Bader analysis [35] of the charge density, before and after CO adsorption to the supported TM atom.

2 Computational details

In this work, the periodic slab approach has been used through. For the computations on the probe molecule, CO, and the isolated MCO reference systems and their cations and anions, a $15 \times 15 \times 15$ Å unit cell has been employed. In all cases, the calculations have been performed in the lower spin state of the system to correlate them with the expected low spin state usually found for adsorbed adatoms on oxide surfaces.

The unreconstructed 1×1 α -Al₂O₃ (0001) surface was represented by a 12-layer thick unit cell consisting of a rhombic prism belonging to the hexagonal system to which periodic 3D conditions were imposed, allowing a vacuum width of 10 Å between the slabs. The model was obtained by truncating the bulk α -Al₂O₃ structure, leaving one Al layer exposed with an oxygen layer right beneath it; this is the generally known as Al-terminated surface. The thickness of the slab is determined by examining the convergence of the surface relaxation against the number of layers [10].

The rutile TiO₂ (110) surface has been modeled with a three-layer slab (nine atomic layers), allowing a vacuum width of 17 Å between the slabs. This vacuum width is considered enough to prevent layer-to-layer interactions. The TM adsorption was computed using a 2×1 supercell obtained by doubling the lattice vector along the [001] direction; this supercell contained 12 Ti and 24 O atoms [31].

DFT calculations under periodic conditions were carried out using the VASP code [36–38] with the projector augmented wave (PAW) method [39, 40]. In these calculations, the energy was obtained using the generalized gradient approximation (GGA) implementation of DFT proposed by Perdew. et al. [41] and a plane with a cutoff of 496 eV for all the calculations. Spin polarization calculations were performed on the open-shell systems. The calculations of the oxide surfaces employed Monkhorst–Pack sets of $6 \times 6 \times 1$ k-points for the α -Al₂O₃ (0001) surface and $4 \times 4 \times 1$ k-points for the TiO₂ rutile (110) surfaces while for the isolated CO molecule and MCO complexes only the Γ -point was included. In all cases, structural minimizations were performed using a conjugated-gradient technique with the residual forces on the atoms being less than 0.05 eV/Å. Vibrational frequencies for adsorbed MCO complexes have been determined freezing all atoms of the oxide support, this is the normal modes of the MCO complex have been uncoupled from the surface phonons. Under this approximation all tested adsorption geometries correspond to minima on their respective potential energy surfaces (PES).

In order to analyze the charge transfer upon adsorption, we have determined the net charge of the adsorbed metals

using the algorithm introduced by Henkelman et al. [42, 43] for the evaluation of the Bader charges [35].

3 Results and discussion

3.1 Isolated monocarbonyls

Infrared spectroscopy of small probe molecules has been used for some time as a experimental tool to study the extent of metal–oxide charge transfer. CO as a probe molecule is of special interest, as its gas phase vibrational frequency may be compared to vibrational frequencies of MCO species and their singly charged ions MCO^+ and MCO^- in rare gas matrices. In those weakly interacting media, the C–O stretching frequencies are found to be deeply sensitive to the charge of the species, which have been related to variations on the extent of CO to metal σ -donation and metal–CO π -back donation [6, 7, 12, 13, 14, 20, 32].

To translate this experimental tool as a computational tool, first we have to validate the procedure by computing the C–O stretching frequencies for the isolated MCO species and their singly charged ions and compare the results obtained with the experimental values for the same species in rare gas matrices. In Table 1, we present the computed geometries, ground state spin multiplicity, C–O stretch vibrational frequencies and shift with respect to the isolated gas phase molecule, for the MCO species and their singly charged ions for the TM atoms M being Cu, Ag, Au, Pd and Pt. Also in this Table 1, we present the experimental frequencies in solid Ne matrix (see [20] and references therein) and the ratio between the experimental CO stretching frequency and the theoretical value, as a measure of the effectiveness of the computational procedure. The average ratios between the experimental and computed C–O vibrational frequencies in metal carbonyls is 1.024 ± 0.016 . This value is better than average ratios obtained for different theoretical procedures [44] that, in general, show that DFT method can provide reasonable predictions for transition–metal–containing compounds.

In order to rationalize the observed trends in the CO vibrational frequencies it is convenient to understand the main components of the metal to CO bonding. The classical Blyholder mechanism [45] usually explains the CO bonding to metal surfaces and atoms in terms of a σ -donation from the CO 5σ orbital to the unoccupied metal orbitals followed by a charge transfer or back-donation from the d_π to the CO $2\pi^*$ unoccupied level. Application of the already mentioned CSOV analysis to study the bonding mechanism and to the CO frequency shifts [19, 46–49] shows that there are two important physical contributions not included in the above scheme. They arise from the

charge superposition of CO and metal orbitals and they lead to large blue shifts. The first one is the Pauli repulsion of the CO lone pair and the metal charge density. The second one is the contribution from the interaction of the CO dipole moment and the metal electric field. This last contribution is small for neutral MCO systems, but significant for charged ones. The remaining contributions to the bonding have a negative contribution to the CO vibrational frequency shift. Of these, the most important is the charge back-donation from the metal d_π to CO π^* . The importance of this effect depends on the metal ionization potential and clearly, the anion will donate more electrons than a neutral metal atom, which in turn will donate more than a cation. This donation will reduce the C–O bonding and, thus, will be the main responsible for the reduction of the C–O stretching frequency.

Following these ideas, in Table 1 it can be observed that the shift in the ν_{CO} stretching frequency is always positive when CO is bonded to a cation (the blue shift resulting from the charge superposition and the Stark effect clearly dominates and there is probably no π -backdonation), while for neutrals and anions the net result is a red-shift of the CO stretching frequency that is larger for anions than for neutrals (the back-donation dominates the bonding mechanism and there is increased back-donation in the anions). Due to its high sensitivity to the electric field of the metal, the ν_{CO} frequency shift is generally large, between $+91.2 \text{ cm}^{-1}$ for AgCO^+ and -365.8 cm^{-1} for CuCO^- . In the case of Pd and Pt, the computed and observed shift for either the cations or the anions are sensibly smaller than those of the coinage metal atoms. However, while this implies that the detailed electronic configuration of the metal affects the ν_{CO} frequency shift, its influence is clearly smaller than the dependence on the charge on the metal.

Some particular cases in MCO complexes presented in Table 1 deserve a special comment. The AgCO^- and AuCO^- negative ions have positive binding energies towards dissociation into their constitutive fragments, that is, they are unstable species. These species have never been experimentally observed. This is due to the closed shell $(n-1)d^{10}ns^2$ configuration of the TM negative atom that reduces the interaction energy on the monocarbonyl anions of the Cu group. In the case of Cu, the interaction energy, although negative with respect to dissociation, is very weak. It may also be possible that these species are Van der Waals minimum on their PES, but the DFT functional does not correctly account for these weak interactions. For silver, the neutral monocarbonyl, AgCO has already a very weak bonding as the d orbitals are very stable relatively to those of Cu and Au, making the π -back donation less efficient. In fact, the neutral AgCO monocarbonyl has not been observed experimentally. Finally, the relativistic effects on Au contract strongly the $6s$ shell and makes these

Table 1 Structural data for CO and the isolated monocarbonyls M-CO (M=Cu, Ag, Au, Pd, and Pt)

M	q	q_M	S	$r_{M-C}/\text{\AA}$	$r_{C-O}/\text{\AA}$	$\langle MCO \rangle$	$\Delta E/eV$	ν_{CO}/cm^{-1}			Shift/ cm^{-1}	
								Calc.	Exp.	Scale	Calc.	Exp.
CO	0	–	<i>s</i>		1.145			2,113.6	2,140.8	1.013		
Cu	1	0.86	<i>s</i>	1.830	1.135	178.3	–1.56	2,201.9	2,234.4	1.015	88.3	93.6
	0	0.18	<i>d</i>	1.861	1.164	142.9	–0.98	1,950.4	2,029.7	1.041	–163.2	–111.1
Ag	1	0.85	<i>s</i>	2.102	1.133	177.5	–0.69	2,204.8	2,233.1	1.013	91.2	92.3
	0	0.12	<i>d</i>	2.191	1.161	133.4	–0.37	1,940.5			–173.1	
Au	–1	–0.68	<i>s</i>	2.388	1.179	114.7	0.26	1,807.6			–306.0	
	1	0.75	<i>s</i>	1.920	1.135	177.4	–1.86	2,192.3	2,236.8	1.020	78.7	96.0
	0	0.05	<i>d</i>	2.002	1.162	140.0	–0.92	1,960.3	2,053.2	1.047	–153.4	–87.6
Pd	–1	–0.65	<i>s</i>	2.233	1.187	118.6	0.02	1,780.0			–333.6	
	1	0.89	<i>d</i>	1.916	1.140	178.5	–1.60	2,134.9			21.3	
	0	0.16	<i>s</i>	1.861	1.162	179.0	–2.30	2,005.1	2,056.4	1.026	–108.5	–84.4
Pt	–1	–0.66	<i>d</i>	1.870	1.187	143.6	–1.60	1,811.7	1,909.0	1.054	–301.9	–231.8
	1	0.91	<i>d</i>	1.829	1.144	180.0	–2.90	2,136.0			22.4	
	0	0.21	<i>s</i>	1.774	1.165	180.0	–3.54	2,023.2	2,065.5	1.021	–90.4	–75.3
	–1	–0.54	<i>d</i>	1.812	1.188	164.7	–2.19	1,867.4	1,896.3	1.015	–246.2	–244.5

Average scale for ν_{CO} on monocarbonyls: 1.024 ± 0.016

q , Total charge of the MCO systems; q_M , charge of M according to a Bader charge analysis; S, spin state of the systems, *s* singlet, *d* doublet; ΔE , binding energy with respect to isolated M and CO fragments

leaves very stable, reducing the strength of the Au–CO interaction. In any case, as these complexes are local minima on their PES, we can obtain the desired parameters (equilibrium geometry and CO vibrational frequency) from our theoretical calculations. A final comment on the data on Table 1 is that the differences found between the computed and the experimental shifts cannot only be assigned to imprecisions on the theoretical calculations. The solid inert gas matrix may have an effect on the experimental shifts of the order of magnitude of these errors.

Figure 1 shows the computed and experimental ν_{CO} frequencies on monocarbonyl systems, correlated to the charge of the MCO complexes. While in almost all cases there is an excellent correlation, to establish a correct relationship, it has to be noted that the charge on the metal center is not necessarily identical to the total charge on the MCO species. According to a Bader charge analysis (see Table 1) the metal atom in neutral MCO complexes is essentially neutral, bearing a positive charge of +0.05 to +0.21 only. The charge of the metal center in MCO^+ complexes is indeed close to the total charge, with values between +0.75 to +0.91. However, for negatively charged MCO^- species the situation is quite different. The total charge of the complex is almost equally shared by the metal center and the carbonyl, with charges on the metal center ranging from –0.54 to –0.68. This means that for neutral or positively charged species, the frequency–charge

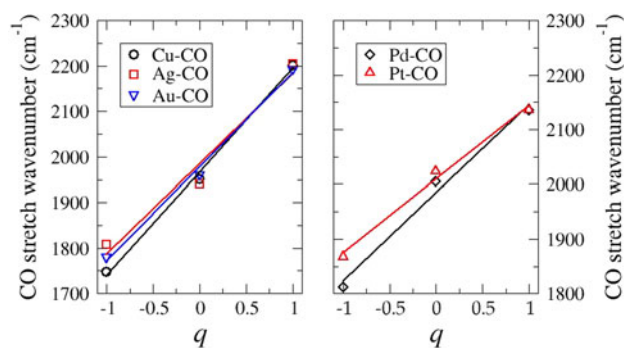


Fig. 1 Linear fitting of the ν_{CO} stretching wavenumber in MCO^q complexes to the complex charge. *Left* Cu, Ag and Au. *Right* Pd and Pt. q is the complex charge

relationship can be used to trace the charge on the metal center, although we can place a error bar of ± 0.1 to 0.2 elementary units on the charge estimated by the use of CO as a probe of the metal center charge. For negatively charged MCO^- systems, however, the error bar that has to be placed on the charge obtained from the frequency shift of the CO stretching mode is larger, between ± 0.4 and 0.5 units of charge. These findings can be rationalized on the basis of the main chemical contributions to the M–CO bonding and the charge displacements that result. On MCO^+ complexes, the σ -donation from the CO 5σ orbital to the M^+ cation will reduce its positive charge, while the π -back donation from the metal d_π orbitals will be limited

by the strong electric field generated by the metal cation. On neutral MCO complexes, the π -back donation from the electron rich d_π orbitals will be a very effective bonding mechanism, resulting in a M atom bearing a slight positive charge. Finally, in MCO^- complexes the π -back donation should be the dominant contribution to the bonding, resulting in an almost equitative distribution of the excess electron density between the M center and the CO molecule.

We can conclude that the computational results reproduce the experimental trend for the observed shift of the frequency of the CO stretching mode in the isolated monocarbonyls and their ions. Moreover, the agreement between the charge that could be assigned to the metal on the basis of the proposed correlation and that resulting from a Bader charge analysis is quantitative for neutral and positively charged M centers. For negatively charged MCO^- complexes the agreement is only semiquantitative, and results should be analyzed with care. A final word of caution is that the presence of an oxide substrate may alter the strength of the Pauli repulsion and the Stark effect, resulting in altered frequency shifts with respect to those of isolated monocarbonyl complexes, even in the absence of a metal-oxide charge transfer.

3.2 Supported metals

Table 2 presents the structural data (bonding distances and MCO angle) as well as the computed CO stretching wavenumber, its shift with respect to free CO, and the metal charge obtained from this shift by interpolating in the straight lines defined by the data for the isolated

monocarbonyls discussed in the previous section of this paper. Metal charges obtained using the Bader approximation are also shown in this Table for comparison and to establish trends.

On the $\alpha\text{-Al}_2\text{O}_3$ (0001) surface, the different adsorption sites are denoted by the symbol of the atom that is below the TM atom and a subindex that indicates the layer to which this atom belongs. The most stable adsorption site for Cu and Ag is the Al_4 site, where the TM atom is coordinated to three O anions of the second layer. This is not the case for Au, Pd, and Pt, for which the strongest metal atom-surface interaction is found at the O_2 site. In the case of Au atom, the data for the metastable Al_4 site are also shown, to rationalize the trend down the coinage metal group. All computed shift are negative, but smaller in absolute value than those found on neutral MCO complexes (see Table 1). This indicates that the charge probed by the CO molecule corresponds to slightly positive metal cations. Effectively, the charge computed for the TM atoms from the ν_{CO} shift is always clearly positive, except for the Au atom adsorbed at the O_2 site that is found to be essentially neutral. For the coinage metal atoms, this is in agreement of previous interpretations of the bonding mechanism for these atoms [9]. In the case of Cu and Ag, the metal adlayer was found to partially reduce the oxide surface, while the main contribution to the bonding in the Au case (at the O_2 adsorption site) was found to be the polarization of the electron cloud of the TM atom towards the surface. Au adsorption at the Al_4 site also results in a partial charge transfer from the TM adlayer to the surface. This is not surprising as any TM atom adsorbed at this site will interact with three low

Table 2 Structural data for CO adsorbed on the supported metals M=Cu, Ag, Au, Pd, and Pt, on the selected surfaces: $\alpha\text{-Al}_2\text{O}_3$ (0001), and TiO_2 (110)

Surface	M	Site	$r_{\text{MC}}/\text{\AA}$	$r_{\text{CO}}/\text{\AA}$	$\angle\text{MCO}$	$\nu_{\text{CO}}/\text{cm}^{-1}$	$\Delta\nu_{\text{CO}}$	q_v	q_M	$q_{\text{M(CO)}}$
$\alpha\text{-Al}_2\text{O}_3$ (0001)	Cu	Al_4	1.781	1.157	180.0	2,073.1	-40.5	0.49	0.34	0.58
	Ag	Al_4	2.002	1.158	180.0	2,036.5	-77.1	0.36	0.21	0.52
	Au	Al_4	1.900	1.161	180.0	2,038.7	-74.9	0.34	0.10	0.48
	Au	O_2	1.975	1.170	146.2	1,989.6	-124.0	0.06	0.05	0.29
	Pd	O_2	1.862	1.159	180.0	2,049.4	-64.2	0.41	0.24	0.59
	Pt	O_2	1.817	1.162	180.0	2,071.2	-42.4	0.41	0.21	0.52
TiO_2 (110)	Cu	Bridge	1.783	1.154	180.0	2,077.4	-36.2	0.51	0.65	0.70
	Ag	Bridge-ang	1.982	1.147	177.5	2,100.1	-13.5	0.58	0.59	0.73
	Au	O	1.873	1.152	180.0	2,112.2	-1.4	0.60	0.27	0.65
	Pd	Bridge-ang	1.867	1.160	180.0	2,018.5	-95.1	0.21	0.34	0.54
	Pt	O	1.817	1.162	180.0	2,040.2	-73.4	0.23	0.34	0.68

q_v , Charge obtained from the ν_{CO} shift; q_M , charge from Bader analysis before CO adsorption; $q_{\text{M(CO)}}$, charge from Bader analysis after CO adsorption

coordinated O anions that try to recover its bulk state by completing their coordination and by taking some charge density from the adsorbed TM atom. Data for Pd and Pt show a significant charge transfer from the TM adlayer to the oxide surface, similar to that found in the Cu/ α -Al₂O₃ system. In the Pd case, this is in agreement with previous studies [8] that, based on cluster models and periodic DFT calculations showed an interaction dominated by the Pd polarization but with a noticeable contribution from the charge transfer from Pd to surface. Similarly, LDA slab calculations on Pt adatoms on the Al₂O₃ (0001) surface [11] show an important amount of charge transfer from the TM atoms to the oxide surface, mainly from the 6s Pt band. Bader charges, computed before and after CO adsorption to the TM/Al₂O₃ system agree substantially with those obtained from the shift in the CO stretching frequency. However, there are details that require some additional comments. The Bader charges computed in absence of adsorbed CO are, in general, ≈ 0.15 – $0.20 e^-$ less than those computed from the CO stretching vibrational shift, while the Bader charges computed after CO adsorption are higher in a similar amount. This behavior can be rationalized by taking into account the numerical errors inherent to the fitting method: the vibrational shift does not strictly follow a linear dependency MCO complexes charge and the charge probed is not strictly the charge of the MCO complex and it has been shown previously. Also, we have to remember that the measure of the charge by using the CO molecule is an indirect method in which the probe modifies the system. Finally, the presence of an oxide substrate will alter the strength of the Pauli repulsion, altering the frequency shift and, thus, the charge obtained for the M center from the fitting procedure.

The amount and direction of the charge transfer at the interface in the Au/TiO₂ catalyst system is still subject of controversy despite the considerable amount of work dedicated to the study of this system. Different papers that have reported on the electronic structure of Au adatoms on the TiO₂ (110) surface [31, 50, 51], have found an almost neutral situation for Au atoms. However, a different work by Wörz et al. [32] dealing with Au atoms supported on TiO₂ films found, on a non defective surface, a strongly bound Au ^{δ^+} -CO, while Au ^{δ^-} -CO complexes are formed on bridging oxygen vacancies. The number of works dealing with the other two member of the group is quite limited. In the work by Giordano et al. [31] the interaction of Cu and Ag with the TiO₂ (110) surface is pictured as strong, with nearly full charge transfer from the TM adatom to the surface based on a Mulliken population analysis and analysis of the atom projected density of states (PDOS). More recent periodic DFT calculations by Rodríguez et al. [52] indicate that Cu adatoms substantially

reduce the TiO₂ surface and bear a significant positive charge ($0.5 e^-$). Our results for the coinage metal atoms show negative shifts and moderately high atomic charges (0.51 – $0.60 e^-$) obtained from the linear fitting of the vibrational frequencies of the MCO complexes. The Bader charges are also high for Cu and Ag, confirming that these two TM partially reduce the support. As it did happen, when the support was Al₂O₃, the adsorption of CO increases the charge reported for the TM adatom. For Au, our results can help to rationalize the different finding previously discussed. The Bader charge analysis shows an Au adatom bearing only a small positive charge before CO adsorption, while both the charge reported by the shift of the CO stretching frequency and the Bader analysis after CO adsorption show a highly charged Au ^{δ^+} -CO complex. It may be possible that the bonding mechanism for isolated Au adatoms is mainly based on the polarization of the TM atom, resulting in a nearly neutral Au atoms. This will be consistent with the small charge transfer reported by the Bader analysis here and in previous works [52], and with the low migration barrier found for these adatoms. [34] Later, the coordination by the CO molecule will repolarize the electronic cloud of the Au atom, resulting in significant charge transfer to the surface and the formation of the Au ^{δ^+} -CO complex. Our results for Pd and Pt adatoms indicate a moderately weak charge transfer from the TM to the surface enhanced, again, upon CO coordination to the metal. For Pd, this confirms previous estimations based on the analysis of the PDOS and CSOV analysis of the bonding mechanism [33]. These tools reveal that Pd deposition is accompanied by a strong polarization of the adatoms that eventually would transfer some electron density towards the surface. The adsorption of Pt atoms has been studied theoretically by Iddir et al. [34], but they offered no clues about the magnitude of the bonding mechanism or the charge transfer that take place upon Pt adsorption. In any case, the stronger adsorption energy found for Pt atoms when compared with Pd atoms will point out to a stronger charge transfer, but their results correspond to a high coverage ($\theta = 0.5$ ML) and an interaction between neighboring Pt atoms cannot be discarded.

In any case, the semiconductor nature of the TiO₂ surface, may result in a sensible modification of the Pauli repulsion, most important in this case than in the α -Al₂O₃ (0001) surface, may explain the larger differences found between the metal charges reported by the CO frequency shift and by the Bader charge analysis. The sensibility of the computed properties of TiO₂ (110) to details details of the model (i.e. number of TiO₂ layers and size of the supercell model), and to the surface coverage allow for further investigation of the electronic properties of the TM/TiO₂ interface.

4 Conclusions

In this paper, we systematically studied the charging of some adsorbed transition metal atoms on two widely used metal oxides surfaces [α -Al₂O₃ (0001) and rutile TiO₂ (110)]. Two procedures are combined to this end: the computed vibrational shift of the CO molecule, that is used as a probe, and the calculation of the atoms charges from a Bader analysis of the electron density of the systems under study. At difference from previous studies that directly compared the vibrational wavenumber of adsorbed CO with that of the gas-phase molecule, we have validated the procedure by comparison of the computed CO stretching wavenumbers in isolated monocarbonyls (MCO) and their singly charged ions with experimental data for these species in rare gas matrices. The agreement found between the computed frequencies and the experimental ones is better than average ratios obtained for different theoretical procedures. Small deviations are observed that can be related to effects of the electronic configuration of the metal, to the fact that the CO molecule is an indirect method of probing the TM charge, and to the influence of the inert gas matrix in the experimental shift. It should be also noted that the charge on the metal center is not necessarily that of the MCO complex. Although the TM atom in neutral and cationic and in MCO complexes the charge of the TM atom is indeed close to the total charge, in MCO⁻ anions the excess electron density is distributed between the TM atom and the CO molecule. Thus, although the computational results correctly reproduce the experimental trend for the observed shift on the CO stretching mode care must be taken for negatively charged complexes as in this case the agreement is only semiquantitative. The transposition of this interpolation scheme to study the extent of metal–oxide charge transfer requires a final caveat: the presence of an oxide substrate may alter the extent of the Pauli repulsion, leading to frequency shift not directly related to a metal–oxide charge transfer. Our results show that while Cu and Ag atoms show a partial charge transfer to the Al₂O₃ surface, this is not the case for Au adatoms, that are basically neutral on the most stable adsorption site. Pd and Pt adatoms also show a significant amount of charge transfer to this surface. On the TiO₂ surface, our results allow an interpretation of previous contradictory data by showing that the adsorption of the probe molecule may repolarize the Au adatoms, that are basically neutral when isolated, and show the presence of highly charged Au ^{$\delta+$} –CO complexes. The other two coinage metal atoms are found to significantly reduce the TiO₂ surface. The combined use of the shift on the vibrational frequency of the CO molecule and the computation of the Bader charges shows to be a useful tool for the study the charge state of adsorbed transition metal atoms and allow to rationalize the

information coming from experimental sources and other complementary tools. In the TiO₂ case the semiconductor nature of the support and the known sensibility of the surface electronic properties to details of the computational model like the number of TiO₂ layers, the degree of surface coverage, and the presence of point defects such as bridging oxygen vacancies allow further investigation of the effects of these parameters on the charge state of adsorbed TM atoms on TiO₂ surfaces.

Acknowledgments This work was funded by the Spanish Ministerio de Educación y Ciencia, MEC (project MAT2008-04918).

References

1. Santra A, Goodman D (2003) *J Phys Condens Matter* 15:R31
2. Fu Q, Wagner T (2007) *Suf Sci Rep* 62:431
3. Campbell CT (1997) *Surf Sci Rep* 27(1–3):1
4. Rainer DR, Xu C, Goodman DW (1997) *J Mol Catal A Chem* 119(1–3):307
5. Freund HJ, Pacchioni G (2008) *Chem Soc Rev* 37(10):2224
6. Frank M, Bäumer M, Kühnemuth R, Freund HJ (2001) *J Phys Chem B* 105(36):8569
7. Judai K, Abbet S, Wörz AS, Heiz U, Giordano L, Pacchioni G (2003) *J Phys Chem B* 107(35):9377–9387
8. Gomes JRB, Illas F, Hernández NC, Márquez A, Sanz JF (2002) *Phys Rev B* 65(12):125414
9. Hernández NC, Sanz JF (2002) *J Phys Chem B* 106(44):11495–11500
10. Hernández NC, Graciani J, Márquez A, Sanz JF (2005). *Surf Sci* 575(1–2):189
11. Verdozzi C, Jennison DR, Schultz PA, Sears MP (1999) *Phys Rev Lett* 82(4):799
12. Zhou M, Andrews L (1999) *J Am Chem Soc* 121:9171
13. Zhou M, Andrews L (1999) *J Phys Chem A* 103:7773
14. Liang B, Zhou M, Andrews L (2000) *J Phys Chem A* 104:3905
15. Sterrer M, Yulikov M, Risse T, Freund HJ, Carrasco J, Illas F, Valentin CD, Giordano L, Pacchioni G (2006) *Angew Chem Int Ed* 45:2633
16. Giordano L, Carrasco J, Valentin CD, Illas F, Pacchioni G (2006). *J Chem Phys* 124(17):174709
17. Niemantsverdriet JW (ed) (2007) *Spectroscopy in catalysis: an introduction*. WILEY-VCH Verlag GmbH & Co., New York
18. Fielicke A, Gruene P, Meijer G, Rayner DM (2009) *Surf Sci* 603(10–12):1427
19. Bagus P, Pacchioni G (2008) *J Phys Conf Ser* 117:012003
20. Zhou M, Andrews L, Charles J, Bauschlicher W (2001) *Chem Rev* 101(7):1931–1962
21. Gomes JRB, Illas F, Hernández NC, Sanz JF, Wander A, Harrison NM (2002) *J Chem Phys* 116(4):1684
22. Nasluzov VA, Rivanenkov VV, Shor AM, Neyman KM, Rösch N (2003) *Chem Phys Lett* 374(5–6):487
23. Rivanenkov VV, Nasluzov VA, Shor AM, Neyman KM, Rösch N (2003) *Surf Sci* 525(1–3):173
24. Gomes JRB, Lodziana Z, Illas F (2003) *J Phys Chem B* 107:6411
25. Meyer R, Ge Q, Lockemeyer J, Yeates R, Lemanski M, Reinalda D, Neurock M (2007) *Surf Sci* 601(1):134
26. Hernández NC, Márquez A, Sanz JF, Gomes JRB, Illas F (2004) *J Phys Chem B* 108:15671
27. Zhou C, Wu J, Kumar TJD, Balakrishnan N, Forrey RC, Cheng H (2007) *J Phys Chem C* 111:13786

28. Bagus PS, Hermann K, Charles J, Bauschlicher W (1984) *J Chem Phys* 80(9):4378
29. Bagus PS, Hermann K, Charles J, Bauschlicher W (1984) *J Chem Phys* 81(4):1966
30. Bagus PS, Illas F (1992) *J Chem Phys* 96(12):8962
31. Giordano L, Pacchioni G, Bredow T, Sanz JF (2001) *Surf Sci* 471(1–3):21
32. Wörz AS, Heiz U, Cinquini F, Pacchioni G (2005) *J Phys Chem B* 109(39):18418
33. Sanz JF, Márquez A (2007) *J Phys Chem C* 111(10):3949
34. Iddir H, Ögüt S, Browning ND, Disko MM (2005) *Phys Rev B* 72(8):081407
35. Bader R (1990) *Atoms in molecules: a quantum theory*. Oxford University Press, New York
36. Kresse G, Hafner J (1993) *Phys Rev B* 47(1):558
37. Kresse G, Furthmüller J (1996) *Comput Mater Sci* 6(1):15
38. Kresse G, Furthmüller J (1996) *Phys Rev B* 54(16):11169
39. Blöchl PE (1994) *Phys Rev B* 50(24):17953
40. Kresse G, Joubert D (1999) *Phys Rev B* 59(3):1758
41. Perdew JP, Chevary JA, Vosko SH, Jackson KA, Pederson MR, Singh DJ, Fiolhais C (1992) *Phys Rev B* 46(11):6671
42. Henkelman G, Arnaldsson A, Jonsson H (2006) *Comput Mater Sci* 36:354
43. Sanville E, Kenny SD, Smith R, Henkelman G (2007) *J Comput Chem* 28:899
44. Ruse E, Johnson D III (2006) NIST Computational Chemistry Comparison and Benchmark Database, NIST Standard Reference Database Number 101. Release 14, September 2006
45. Blyholder G (1964) *J Phys Chem* 68:2772
46. Illas F, Zurita S, Rubio J, Márquez AM (1995) *Phys Rev B* 52(16):12372
47. Bagus PS, Pacchioni G (1990) *Surf Sci* 236(3):233
48. Illas F, Zurita S, Márquez AM, Rubio J (1997) *Surf Sci* 376(1–3):279
49. Bagus PS, Miller W (1985) *Chem Phys Lett* 115(6):540
50. Chrétien S, Metiu H (2007) *J Chem Phys* 127(8):084704
51. Graciani J, Nambu A, Evans J, Rodríguez JA, Sanz JF (2008) *J Am Chem Soc* 130(36):12056
52. Rodríguez JA, Evans J, Graciani J, Park JB, Liu P, Hrbek J, Sanz JF (2009) *J Am Chem Soc* 131(17):7364